processes

MDPI

Article

Carbon Functionalized Material Derived from Byproduct of Plasma Tar-Cracking Unit on Biomass Gasifier Collected Using Standard Impinger Method

Harry Poetra Soedarsono [1], Ferry Faizal [1,2], Camellia Panatarani [1,2] and I Made Joni [1,2,*]

[1] Department of Physics, Faculty of Mathematic and Natural Sciences, Universitas Padjadjaran, Jl. Raya Bandung-Sumedang, Km 21, Jatinangor, Sumedang 45363, Indonesia
[2] Functional Nano Powder University Centre of Excellence (FiNder U CoE), Universitas Padjadjaran, Jl. Raya Bandung-Sumedang, Km 21, Jatinangor, Sumedang 45363, Indonesia
* Correspondence: imadejoni@phys.unpad.ac.id

Abstract: Reduction of tar concentration in biomass gasification with secondary plasma tar cracking unit remains a challenge to meet the requirement for clean syngas energy applications. Typically, the post-treatment of syngas to reduce the tar from an updraft fixed-bed reactor is using secondary plasma tar cracking unit. In this study, an additional trapping train was introduced as a mechanism to harvest byproducts of the tar decomposition process (byproduct carbon functionalized material or BCFM). The measurement in gravimetric and particle size distribution, supported by photoluminescent (PL) and Fourier transform infrared spectroscopy (FT–IR) of BCFM, were conducted to reveal the BCFM characteristic. The gravimetric analysis showed that the application of the secondary plasma tar cracking unit highly reduced the tar concentration. Similarly, the average particle size also decreased significantly. The peak emission spectra of the suspended BCFM particle under the plasma cracking treatment shifted from around 500 nm to around 400 nm. The significant changes in the BCFM functional group occurred due to the successful cracking process. It was concluded that the byproduct received from the plasma cracking process resulted in very low tar content and was revealed to be a carbon functionalized material with a very small size (16.2 nm) and stable suspension.

Keywords: gasification; plasma; tar cracking; carbon; functionalized material

Citation: Soedarsono, H.P.; Faizal, F.; Panatarani, C.; Joni, I.M. Carbon Functionalized Material Derived from Byproduct of Plasma Tar-Cracking Unit on Biomass Gasifier Collected Using Standard Impinger Method. *Processes* **2022**, *10*, 1733. https://doi.org/10.3390/pr10091733

Academic Editor: Angela Scala

Received: 20 July 2022
Accepted: 26 August 2022
Published: 1 September 2022

1. Introduction

A technique for generating alternative, environmentally acceptable fuels for power generation is biomass gasification. Solid biomass is transformed into useful synthetic gases or syngas comprised of H_2 and CO using an indirect combustion process [1]. Drying, pyrolysis, and partial oxidation are the order in which the decomposition of biomass occurs during gasification [2]. Due to incomplete conversion of the liquid products generated by the pyrolysis process, the final product gas contains tar compounds. Tar formation is a severe problem in gasification systems. It causes issues such as clogging in filter pores and cold spots due to coke formation and condensation. Tar in the syngas is considered the Achilles' heel of gasification [3].

There are several methods for reducing tar concentration in syngas, including catalytic cracking, thermal cracking, condensation, and several others. Plasma cracking is one way to reduce tar in syngas. Both primary and secondary plasma tar cracking systems contain enough energy to initiate tar decomposition reactions. The methods showed promising results in the tar reduction process [4]. Interestingly, recent studies show biomass and coal tar pitch as precursors in synthesizing functionalized carbon quantum dots (CQDs) [5,6]. CQDs can be synthesized using various methods, including hydrothermal, carbonization, microwave irradiation, and chemical oxidation [7,8]. Hsu et al. discovered CD with a diameter of 5 nm synthesized from coffee grounds using a hydrothermal method [9].

Ding et al. discovered that CQDs synthesized from various crop biomasses using the hydrothermal method exhibit strong blue fluorescence properties [10]. Previous studies also show that a small amount of tar is still present in the syngas after plasma treatment [11,12]. Therefore, to further functionalize the remaining tar, it is necessary to characterize it. This study aims to investigate the impact of secondary plasma tar cracking unit power on tar concentration of syngas and also to characterize the byproduct of the tar decomposition process (byproduct carbon functionalized material or BCFM) trapped using the standard impinger method.

2. Materials and Methods

This research was conducted by utilizing the updraft gasification reactor type, which comprises the advantage of easy construction and high thermal efficiency, with a maximum capacity of 1 kg [13]. Corncobs were used in this study as raw materials that had previously been processed through a hammer mill to obtain chunks with relatively uniform size. Smaller corncobs (around 6.7–25 mm in diameter) are required for more reactive biomass. This size range promotes higher efficiency in the gasification process [14].

The Secondary Plasma Tar Cracking Unit used in this experiment consists of a high voltage generator and a plasma chamber. A high voltage generator consists of a 12 V power supply, oscillator module, and flyback transformers. Schematic diagrams of the high voltage generator circuit can be found in Figure 1a,b. Figure 1a can generate a voltage up to 12 kV using 42 Watt of power. Similarly, Figure 1b shows two circuits in Figure 1a connected in parallel at the output, which produces the same voltage (12 kV), but with power doubled (85 Watts). Plasma chambers are made of fire bricks with a hole that has a radius of 3 mm. There are two electrodes with a graphite material, which are placed 4 mm apart. This is shown schematically in Figure 1c,d.

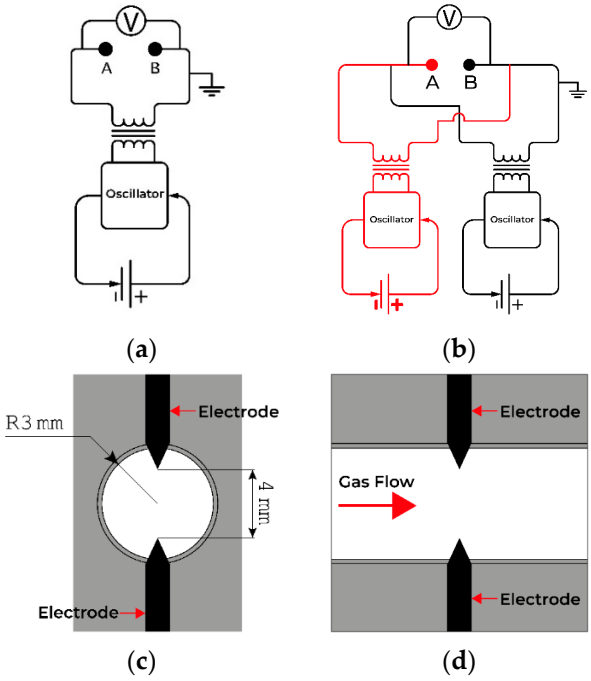

Figure 1. Diagram of a high voltage circuit with 42 Watts of power (**a**) and 85 Watts of power (**b**), and diagram of the plasma chamber, showing the front (**c**) and side (**d**).

In this experiment, the trapping method was adapted from UNI EN 15,439—2008 [15]. As illustrated in Figure 2, a trapping train of six impinger bottles was used. The trapping train also included a flowmeter and vacuum pump. A 10 L min^{-1} flow rate was set, and a vacuum pump was used to draw the syngas.

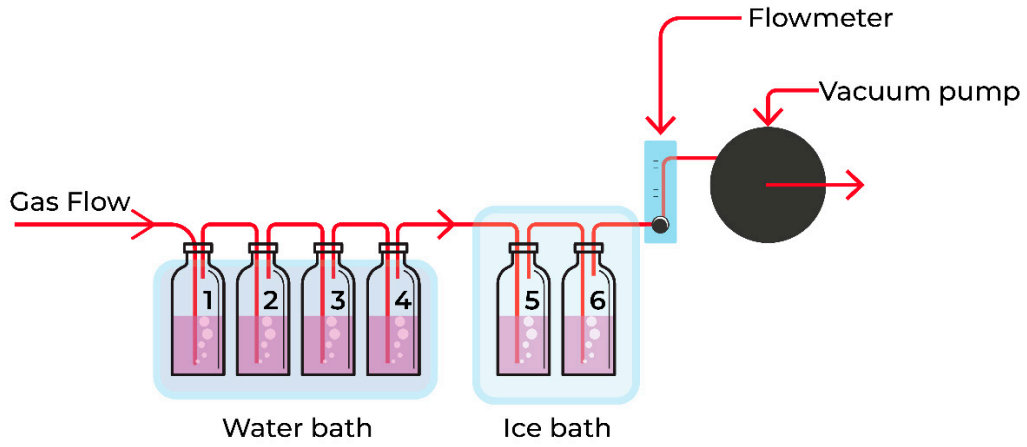

Figure 2. Sampling train schematic diagram.

Furthermore, acetone was used as a solvent. The first to fourth impinger bottles were placed in a water bath at about 20 °C and filled with 50 mL of acetone. The fifth and sixth impinger bottles were placed in an ice bath at about −17 °C. After 10 min of sampling (equivalent to 100 L syngas), measurements were made on every impinger bottle.

A schematic of the experiment is illustrated in Figure 3. The experiment was conducted with three different plasma power levels. A plasma power of 0 W was used as a control and 42 Watts and 85 Watts as experimental conditions. Details on experimental conditions are shown in Table 1.

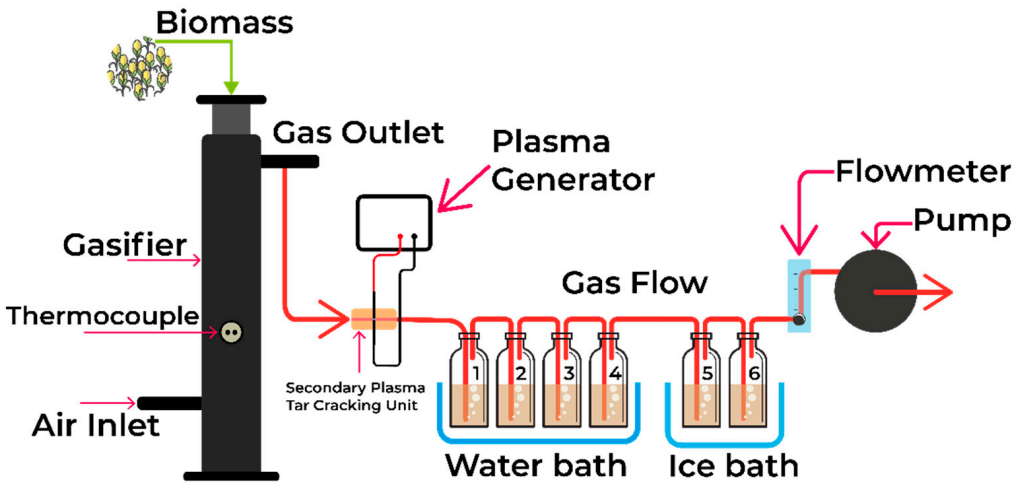

Figure 3. Experimental setup.

Table 1. Experimental condition.

Parameter	0 W	42 W	85 W
Reactor type	Updraft	Updraft	Updraft
Biomass	Corncob	Corncob	Corncob
Reactor temperature	828 °C	783 °C	775 °C
Water bath temperature	22.3 °C	21.5 °C	20.5 °C
Ice bath temperature	−17.4 °C	−15.7 °C	−18.7 °C
Sampling time	600 s	600 s	600 s
Flow rate	10 L min^{-1}	10 L min^{-1}	10 L min^{-1}
Solvent	Acetone	Acetone	Acetone

Samples of tar collected were then characterized by Fourier Transform Infrared Spectroscopy (FT–IR), Photoluminescence Spectroscopy (PL), Particle Size Analyzer (PSA), and Gravimetric Analysis. The chemical structure of tar was investigated with FT–IR spectroscopy. A small sample from each impinger bottle was analyzed. IR spectra were obtained in the range of 4000–500 cm^{-1}. Luminescence properties of tar samples were also analyzed using Photoluminescence spectroscopy. The measurements were carried out for every impinger bottle using an excitation wavelength of 254 nm. Furthermore, PSA was used to investigate the effect of plasma on the size distribution of the tar particles trapped in the impinger. Gravimetric analysis was conducted in this study to determine the tar concentration in syngas quantitatively. Following the procedure, the contents of all impinger bottles were mixed in a beaker glass and heated to 60 °C. Within six hours, the solvent, which has a low boiling point (56 °C), would boil and leave a residue. Then, the beaker glass with tar residue was weighed. The difference between it and an empty beaker glass was defined as the tar concentration on the syngas.

3. Results and Discussions

3.1. Gravimetric Analysis

Gravimetric test results are shown in Table 2. According to the gravimetric test, plasma significantly reduced the result of tar concentration in syngas. The tar concentration in syngas without plasma was 0.0562 g L^{-1}. When syngas was exposed to plasma, the BCFM concentration in the syngas decreased significantly to 0.0221 g L^{-1} and 0.0073 g L^{-1}, correspondingly for the plasma power of 42 and 85 W. Therefore, an increase in plasma power significantly reduced the BCFM concentration. This performance is in line with previous studies utilizing plasma tar cracking secondary units with a tar cracking efficiency of 86–99% [12].

Table 2. The effect of plasma on tar concentration.

Plasma Power (W)	Tar Concentration (g L^{-1})
0	0.0562
42	0.0221
85	0.0073

3.2. Particle Size Distribution Analysis

We measured the size distribution of tar and BCFM particles on each impinger bottle (1–6) at different plasma powers. As can be seen in Figure 4a, there is a difference in the average tar particle size across all impinger bottles. Impinger–1 in the control sample has a z–average value of 2301.1 nm; the z–average value then decreases to impinger–6 with a z–average value of 836.5 nm.

A decrease in particle size can also be seen in Figure 4b,c, where the peak of the particle size distribution shifted to a smaller diameter value when the plasma cracking unit was applied. Figure 4b shows that the BCFM average particle size for each impinger decreased significantly when the plasma power of 42 Watts was applied compared to without power (control samples). The z–average value for impinger–1 is 306.7 nm, and for impinger–2 is 58.6 nm. The presence of large particles such as ash in impinger–1 may cause a significant difference in z–average values between impinger–1 and impinger–2. However, the z–average of impinger–5 and impinger–6 were significantly increased to 606.1 nm and 1003.5 nm, respectively. The presence of a new peak on the higher size indicated that the BCFM particles were agglomerated, as shown in Figure 4b. Figure 4c also shows a decrease in BCFM average particle size. When plasma power was doubled to 85 Watts, the z–average on impinger–1 decreased to 137.2 nm. It was highlighted that suspended BCFM particles in impinger–5 and impinger–6 did not exhibit agglomeration. Interestingly, very small particles were obtained in both suspended BCFM particles of impinger–5 and impinger–6, correspondingly with z–average of 37.8 and 16.2 nm. This result showed that plasma power plays an important role in decreasing suspended BCFM average particle size.

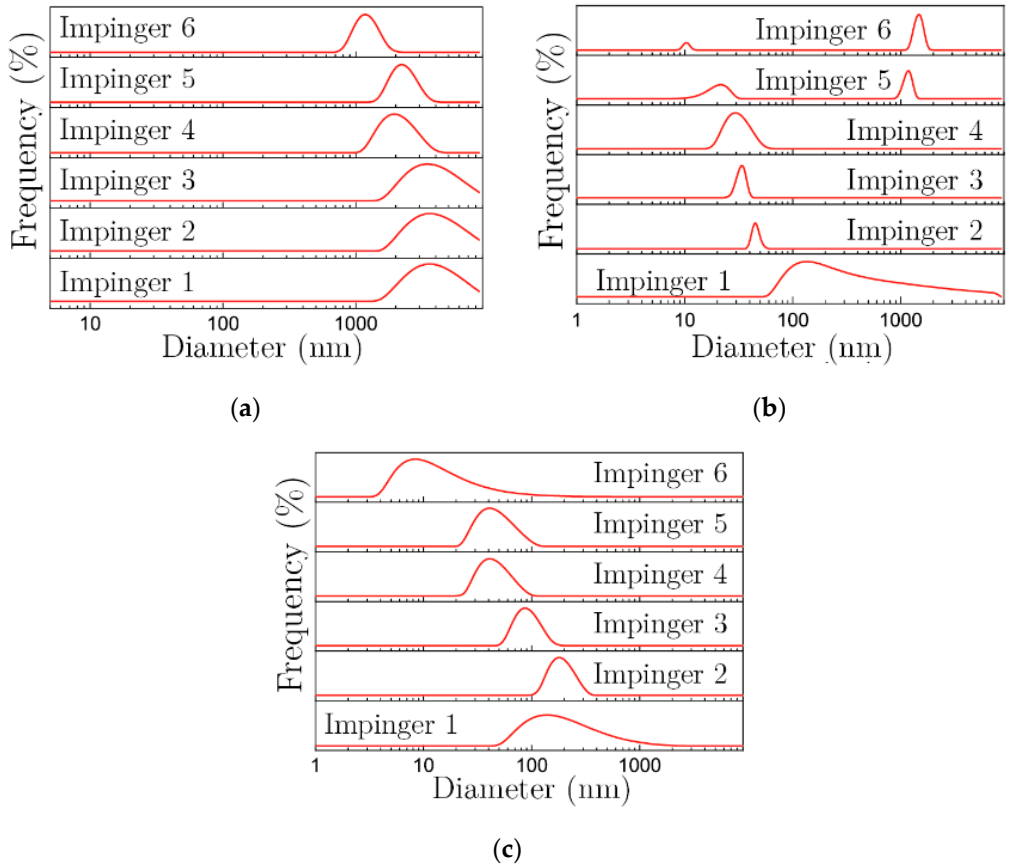

Figure 4. The effect of different plasma powers. (**a**) 0 Watts, (**b**) 42 Watts, and (**c**) 85 Watts on the particle size distribution of tar (0 W) and BCFM (42 and 85 W) in impinger 1–6.

3.3. Photoluminescence Spectroscopy Analysis

The luminescence properties of tar and BCFM particles can be analyzed using PL spectroscopy. In the control sample (Figure 5a), the emission spectra on impinger–1–impinger–6 shift from 500 nm to 404 nm with increasing impinger number. Similarly, this shift can be observed in BCFM samples with a plasma power of 42 watts and 85 watts. For BCFM samples exposed to 42 Watts plasma power (Figure 5b), the emission spectra also shift from 486 nm in impinger–1 to 395 nm in impinger–5. Moreover, for samples exposed to 85 Watts plasma power (Figure 5c), the emission spectra also shift from 490 nm in impinger–1 to 403 nm in impinger–4. The shift in emission peak is possibly due to the smaller BCFM particle size known as the quantum size effect as a result of the plasma cracking process. Additionally, the shift can also be caused by the functional groups within the BCFM that change under the influence of plasma, which will be discussed later using FTIR analysis. The emission spectra in Figure 5b,c impinger–5 and impinger–6 were similar to previous studies of carbon quantum dots derived from biomass tar [10].

3.4. Fourier Transform—Infrared Spectroscopy Analysis

There is a difference in the IR spectrum between impinger 1 and 6. Figure 6a shows the IR spectrum for tar and BCFM samples in impinger–1. The broadband between 3250 and 3500 cm^{-1} with a peak at 3400 cm^{-1} corresponds to O–H stretching, which indicates the presence of alcohol and phenol [16]. The effect of plasma can be seen more clearly in the BCFM sample on impinger–6 (Figure 6b). The intermolecular bonds between the oxygen and hydrogen were no longer visible on impinger–6 on BCFM samples with plasma power 42 and 85 W, indicated by the disappearance of peaks between 3250 and 3500 cm^{-1}. The peak at 2950 cm^{-1} can be seen in Figure 6a and also corresponds to O–H stretching bond

between the atoms. This particular bond clearly disappeared under the effect of plasma, as shown in Figure 6b.

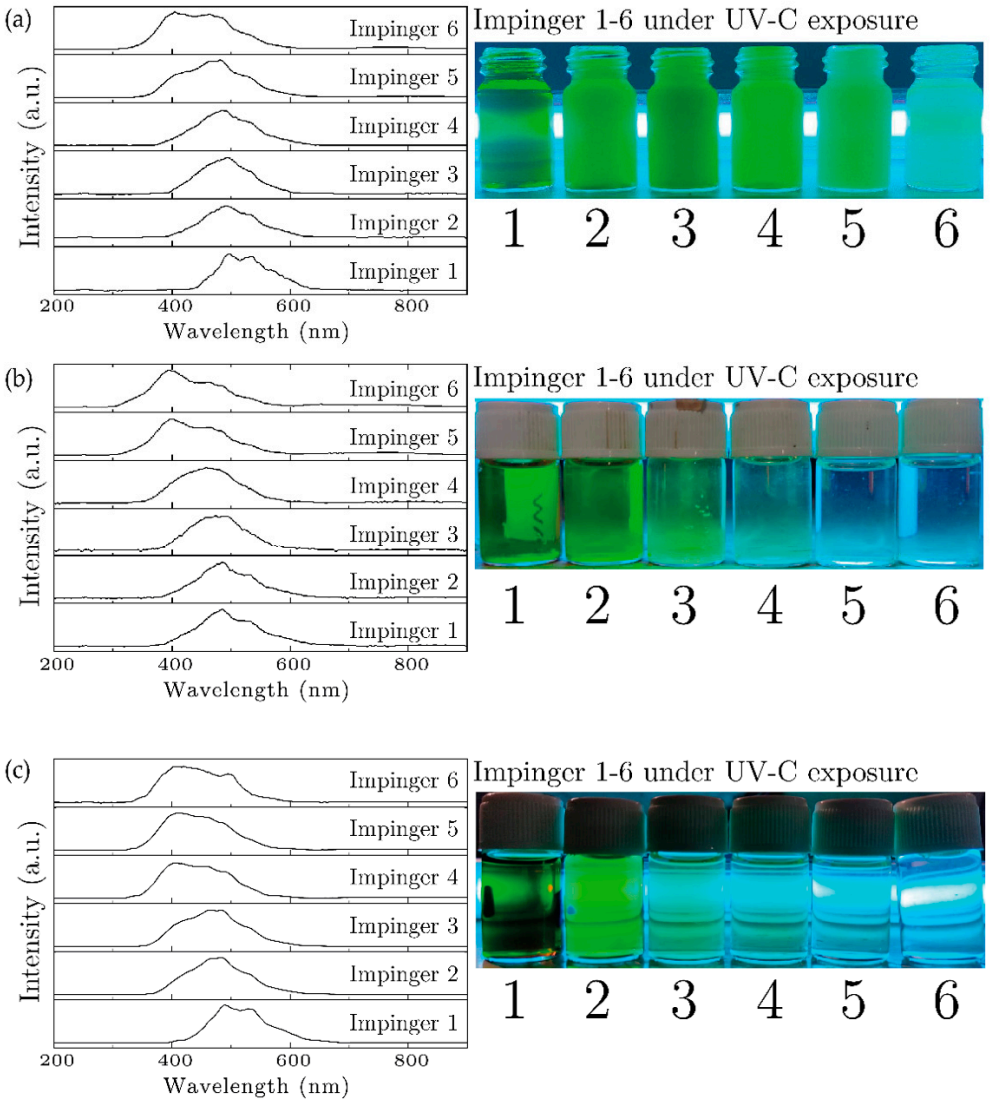

Figure 5. The effect of different plasma powers: 0 Watts (**a**), 42 Watts (**b**), 85 Watts (**c**) on the emission spectrum of tar in impinger 1–6.

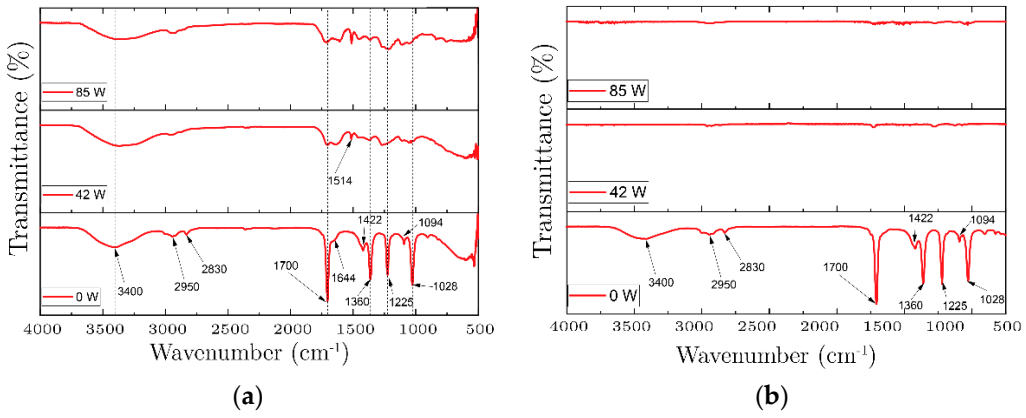

Figure 6. IR spectrum on impinger–1 (**a**) and IR spectrum on impinger–6 (**b**).

The peak at 2830 cm^{-1} and 1700 cm^{-1} correspond to C–H and C=O bonds, respectively, which indicates the presence of aldehyde and conjugated aldehyde in the tar samples. The presence of the C=O bond in BCFM samples is responsible for the green luminescence colour [17]. The C–H bond did not significantly change due to the presence of plasma. Interestingly, the peaks corresponding to C=O bonds decreased significantly when plasma was applied, as shown in Figure 6a. The peak at 1514 cm^{-1} in BCFM samples corresponds to the N–O bond, indicating the presence of nitro compounds. The reaction between Nitrogen and Oxygen occurs because plasma consists of free radicals, electrons, ions, and excited molecules (highly reactive environment) [4]. A similar condition also increases the probability of tar chemical bond breaking. For example, the peak at 1644 cm^{-1} (correspond to C=C bond in tar) decreased significantly under the influence of 42 and 85 W plasma power (Figure 6b). At 1422, 1360, 1225, 1094 cm^{-1}, the peaks correspond to the O–H and C–O functional groups, which also decrease under the influence of plasma. The peak at 1028 cm^{-1} corresponds to the C–N functional group, which is responsible for blue luminescence in BCFM samples [18]. It is highlighted that the BCFM trapped in impinger–6 for both 42 and 85 W plasma powers possesses very low tar content due to the success of the secondary plasma tar cracking unit. Remarkably, the obtained byproduct was revealed to be a carbon–functionalized material with a very small size (16.2 nm) and well-dispersed suspension. Upon further analysis of particle size distribution, luminescence properties, and the various types of bonds that comprise the BCFM, it is verified that the luminescence phenomenon in BCFM particles is caused by a combination of the quantum size effect and the presence of the surface state in BCFM particle [19].

4. Conclusions

The increase of secondary plasma tar cracking unit power substantially impacts the BCFM characteristics during the cracking process. Plasma power affects not only the concentration of BCFM in syngas but also its size distribution, luminescence properties, and molecular structure. Gravimetric results show a significant reduction in BCFM concentration. The change in particle size distribution was confirmed by tests using a particle size analyzer with a 16.2 nm z–average after plasma treatment.

Further, plasma treatment also alters the BCFM luminescence properties, with the emission peak shifting towards a blue colour in different impinger bottles. This shift in emission peaks occurs due to the changes in the particle size distribution of BCFM on every impinger bottle. The FT–IR result shows that the peaks changed significantly before and after plasma treatment, indicating a change in BCFM molecular structure. These results show that the byproduct of the secondary plasma tar cracking unit was revealed to be a carbon functionalized material with a very small size (16.2 nm) and well-dispersed suspension.

Author Contributions: Conceptualization, H.P.S., F.F. and I.M.J.; methodology, H.P.S. and F.F.; validation, C.P. and I.M.J.; formal analysis, H.P.S. and F.F.; resources, I.M.J. and C.P.; data curation, C.P.; writing—original draft preparation, H.P.S.; writing—review and editing, F.F., I.M.J. and C.P.; visualization, H.P.S.; supervision, F.F., C.P. and I.M.J. All authors have read and agreed to the published version of the manuscript.

Funding: This work was funded by Academic Leadership Grant, contract number 2203/UN6.3.1/PT.00/2022.

Institutional Review Board Statement: Not applicable.

Informed Consent Statement: Not applicable.

Data Availability Statement: The data presented in this study are available in this article.

Conflicts of Interest: The authors declare no conflict of interest.

References

1. Bosmans, A.; Vanderreydt, I.; Geysen, D.; Helsen, L. The Crucial Role of Waste-to-Energy Technologies in Enhanced Landfill Mining: A Technology Review. *J. Clean. Prod.* **2013**, *55*, 10–23. [CrossRef]
2. Ruiz, J.A.; Juárez, M.C.; Morales, M.P.; Muñoz, P.; Mendívil, M.A. Biomass Gasification for Electricity Generation: Review of Current Technology Barriers. *Renew. Sustain. Energy Rev.* **2013**, *18*, 174–183. [CrossRef]
3. Saleem, F.; Harris, J.; Zhang, K.; Harvey, A. Non-Thermal Plasma as a Promising Route for the Removal of Tar from the Product Gas of Biomass Gasification—A Critical Review. *Chem. Eng. J.* **2020**, *382*, 122761. [CrossRef]
4. Rueda, Y.G.; Helsen, L. The Role of Plasma in Syngas Tar Cracking. *Biomass Convers. Biorefinery* **2020**, *10*, 857–871. [CrossRef]
5. Malavika, J.P.; Shobana, C.; Sundarraj, S.; Ganeshbabu, M.; Kumar, P.; Selvan, R.K. Green Synthesis of Multifunctional Carbon Quantum Dots: An Approach in Cancer Theranostics. *Biomater. Adv.* **2022**, *136*, 212756. [CrossRef] [PubMed]
6. Hu, C.; Zhu, Y.; Zhao, X. On-off-on Nanosensors of Carbon Quantum Dots Derived from Coal Tar Pitch for the Detection of Cu2+, Fe3+, and L-Ascorbic Acid. *Spectrochim. Acta—Part A Mol. Biomol. Spectrosc.* **2021**, *250*, 119325. [CrossRef] [PubMed]
7. de Oliveira, B.P.; da Silva Abreu, F.O.M. Carbon Quantum Dots Synthesis from Waste and By-Products: Perspectives and Challenges. *Mater. Lett.* **2021**, *282*, 128764. [CrossRef]
8. Vinoth Kumar, J.; Kavitha, G.; Arulmozhi, R.; Arul, V.; Singaravadivel, S.; Abirami, N. Green Sources Derived Carbon Dots for Multifaceted Applications. *J. Fluoresc.* **2021**, *31*, 915–932. [CrossRef] [PubMed]
9. Hsu, P.C.; Shih, Z.Y.; Lee, C.H.; Chang, H.T. Synthesis and Analytical Applications of Photoluminescent Carbon Nanodots. *Green Chem.* **2012**, *14*, 917–920. [CrossRef]
10. Ding, S.; Gao, Y.; Ni, B.; Yang, X. Green Synthesis of Biomass-Derived Carbon Quantum Dots as Fluorescent Probe for Fe3+ Detection. *Inorg. Chem. Commun.* **2021**, *130*, 108636. [CrossRef]
11. Materazzi, M.; Lettieri, P.; Mazzei, L.; Taylor, R.; Chapman, C. Tar Evolution in a Two Stage Fluid Bed-Plasma Gasification Process for Waste Valorization. *Fuel Process. Technol.* **2014**, *128*, 146–157. [CrossRef]
12. Materazzi, M.; Lettieri, P.; Taylor, R.; Chapman, C. Performance Analysis of RDF Gasification in a Two Stage Fluidized Bed-Plasma Process. *Waste Manag.* **2016**, *47*, 256–266. [CrossRef] [PubMed]
13. Nurhilal, O.; Faizal, F.; Soedarsono, H.P. Pengaruh Laju Aliran Udara Terhadap Konsentrasi Kandungan Gas Mampu Bakar dan Daya Gasifikasi. *J. Ilmu Inov. Fis.* **2019**, *3*, 84–90.
14. Oveisi, E.; Sokhansanj, S.; Lau, A.; Lim, C.J.; Bi, X.; Ebadian, M.; Preto, F.; Mui, C.; Gill, R. In-Depot Upgrading the Quality of Fuel Chips for a Commercial Gasification Plant. *Biomass Bioenergy* **2018**, *108*, 138–145. [CrossRef]
15. Dafiqurrohman, H.; Bagus Setyawan, M.I.; Yoshikawa, K.; Surjosatyo, A. Tar Reduction Using an Indirect Water Condenser and Rice Straw Filter after Biomass Gasification. *Case Stud. Therm. Eng.* **2020**, *21*, 100696. [CrossRef]
16. Zubair Yahaya, A.; Rao Somalu, M.; Muchtar, A.; Anwar Sulaiman, S.; Wan Daud, W.R. Characterization of Tar Formation during High Temperature Gasification of Different Chemical Compositions in Biomass. In *Proceedings of the IOP Conference Series: Earth and Environmental Science*; Institute of Physics Publishing: Bristol, UK, 2019; Volume 268.
17. Yu, J.; Liu, C.; Yuan, K.; Lu, Z.; Cheng, Y.; Li, L.; Zhang, X.; Jin, P.; Meng, F.; Liu, H. Luminescence Mechanism of Carbon Dots by Tailoring Functional Groups for Sensing Fe^{3+} Ions. *Nanomaterials* **2018**, *8*, 233. [CrossRef] [PubMed]
18. Vercelli, B.; Donnini, R.; Ghezzi, F.; Sansonetti, A.; Giovanella, U.; la Ferla, B. Nitrogen-Doped Carbon Quantum Dots Obtained Hydrothermally from Citric Acid and Urea: The Role of the Specific Nitrogen Centers in Their Electrochemical and Optical Responses. *Electrochim. Acta* **2021**, *387*, 138557. [CrossRef]
19. Tyutrin; Wang, R.; Martynovich, E.F. Luminescent Properties of Carbon Quantum Dots Synthesized by Microplasma Method. *J. Lumin.* **2022**, *246*, 118806. [CrossRef]